

Electroencephalogram denoising using discrete wavelet transform and adaptive noise cancellation based on information theory

Hashem Abdolahi¹, Ali Akbar Khazaei¹, Mahdi Azarnoosh², Seyed Ehsan Razavi¹

¹Department of Electrical Engineering, Mashhad Branch, Islamic Azad University, Mashhad, Iran

²Department of Biomedical Engineering, Mashhad Branch, Islamic Azad University, Mashhad, Iran

Article Info

Article history:

Received Jan 23, 2024

Revised Sep 17, 2024

Accepted Sep 30, 2024

Keywords:

Adaptive noise cancellation

Discrete wavelet transform

Error entropy

Information theory

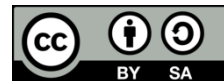
Mean squared error

Noise reduction

ABSTRACT

One of the most frequently used techniques for removing background noise from electroencephalogram (EEG) data is adaptive noise cancellation (ANC). Nonetheless, there exist two primary disadvantages associated with the adaptive noise reduction of EEG signals: the adaptive filter, which is supposed to be an approximation of contaminated noise, lacks the reference signal. The mean squared error (MSE) criterion is frequently employed to achieve this goal in adaptive filters. The MSE criterion, which only considers second-order errors, cannot be used since neither the EEG signal nor the EOG artifact are Gaussian. In this work, we employ an ANC system, deriving an estimate of EOG noise with a discrete wavelet transform (DWT) and input this signal into the reference of the ANC system. The entropy-based error metric is used to reduce the error signal instead of the MSE. Results from computer simulations demonstrate that the suggested system outperforms competing methods with respect to root-mean-square-error, signal-to-noise ratio, and coherence measurements.

This is an open access article under the [CC BY-SA](#) license.



Corresponding Author:

Ali Akbar Khazaei

Department of Electrical Engineering, Mashhad Branch, Islamic Azad University

Mashhad, Iran

Email: khazaei@mshdiau.ac.ir

1. INTRODUCTION

Electroencephalogram (EEG) signal is referred to as measurements of electrical activity of the brain, which is performed by electrodes placed over the scalp. Blinking or moving the head while recording the EEG signal can lead to contamination of the signal with the electrooculogram (EOG) artifact. In many applications used in EEG, like the brain-computer interface (BCI), the existence of artifacts within the EEG signal diminishes the efficiency of the system [1]. Therefore, the elimination of artifacts is crucial in EEG signal analysis.

Regression-based techniques find applications in two distinct domains, time and frequency [2], [3], for omitting EOG artifact of EEG signal, which is recorded for likely provoked studies. In these methods, we can use EEG data which is graded for different causes for obtaining the mean coefficients of transmission within each EEG channel and EOG. However, within the process, the mean transfer coefficients for removing EOG from real-time EEG signals is insufficient because EOG and EEG signals exhibit dynamic characteristics. Hence, the necessity for adaptive filters arises in order to monitor the dynamic alterations in the signal [4].

The utilization of adaptive noise cancellation (ANC) in biomedical signals is extensive [5]–[8]. Nevertheless, these methods typically presuppose the availability of a referenced signal for ANC. An alternative approach employs an adaptive noise reduction method with self-contained component analysis [9].

This involves the application of independent component analysis (ICA) on EEG signals proximate to the eye (F_p1 or F_p2) to derive active noise cancellation basis signals. It should be noted that this method can be applied solely to multiple-electrode EEG signal analysis so, as a result may not be suitable for portable devices.

The local singular spectrum analysis (SSA) method [10], [11] has found application in the elimination of high-level EOG artifacts from single-channel EEG signals [12], [13]. Through the proposed method, vectors of feature are generated through sorting of delayed signals, followed by clustering using the K-means algorithm [14]. Additionally, in the process of singular value decomposition, we calculate the eigenvectors and eigenvalues of the covariance matrix for each category. The minimum description length (MDL) metric [15] quantifies the data necessary for estimating EOG signal, considering the dimension of signal subcategory or the number of eigenvectors. It's important to emphasize that achieving an accurate estimate of the signal subcategory requires creating sufficient separation among the eigenvalues that define EEG and EOG signals [10].

Effectiveness of the local SSA approach primarily lies in its capability to clean frontal EEG signals from EOG interference, in situations characterized by a substantial rise in EOG amplitude within the EEG. In contrast, EEG signals are typically most reliable at channels C3 and C4 [10], and due to the spatial separation between the electrodes and the eye, there isn't a substantial magnitude contrast among the eigenvalues presenting EEG and EOG signals. Consequently, MDL criterion may fall short in accurately estimating the true dimension for the signal subcategory, leading to residual EOG artifacts in the denoised EEG signal.

An adaptive line enhancer (ALE) was employed for separating the electrocardiogram (ECG) and electromyogram (EMG) based on the principles of SSA [16]. In this approach, the ALE is designed to exclusively eliminate the interference signal by utilizing the cyclic nature of the artifact and its delayed version, with the delay determined according to the periodicity of the corrupted signal. Nonetheless, given that EEG and EOG signals are inherently dynamic, the presented approach demonstrates limited effectiveness in the elimination of EOG artifacts from EEG signals.

Combination of discrete wavelet transform (DWT), and ANC has been used to cut out EOG artifact from EEG signals [17]. Through the method, the DWT is applied to the EEG signal to obtain the EOG basis signal, then the EOG artifact is dynamically deleted from the EEG signal. It is quite clear that the type of wavelet function and figure of disintegration levels are important for a good estimate of the reference signal. The efficiency of this method primarily relies on estimation of the reference signal.

The majority of algorithms employed for error reduction in adaptive filters rely on the mean squared error (MSE) measure. However, it's important to note that the MSE criterion is primarily suitable for Gaussian and stationary signals as it solely takes into account the mean and variance of the error distribution. This criterion may not yield an optimal response for signals that exhibit non-Gaussian characteristics or contain significant information in their higher-order statistics [3].

If the probability density function (PDF) of the error is non-Gaussian, then an appropriate cost function for the adaptive filter must be used. Erdogmus and Principe [18] have used the error entropy criterion in a non-linear adaptive system. So far, many algorithms like minimum error entropy with stochastic information gradient (MEE-SIG) [19], minimum error entropy with self adjusting step-size (MEE-SAS) [20], and normalized minimum error entropy (NMEE) [21], have been presented based on this criterion. When the goal of adaptation is to remove uncertainty from the error signal as much as feasible, the error entropy criterion is preferable to the MSE criterion [3].

Algorithms that operate on the principle of error entropy tend to exhibit high resilience against outliers, non-Gaussian, and non-stationary noise sources. Consequently, these algorithms prove to be particularly well-suited for effectively eliminating EOG artifacts from EEG signals, as both the EEG signal and EOG artifact exhibit characteristics that are neither Gaussian nor stationary. Also, the entropy-based error criterion considers the higher-order statistical conduct of the systems and signals [3].

In the proposed approach, we introduce the DWT-MEE algorithm for removing EOG artifacts from EEG signals. Conventional least mean squares (LMS) algorithm may not possess the optimal capability to accurately track EOG artifacts due to their non-Gaussian characteristics. Furthermore, minimum error entropy (MEE) method represents a substantial improvement over the LMS algorithm, primarily because it constrains error entropy rather than solely focusing on mean and variance considerations [3].

In the suggested approach, an estimation of the EOG interference is derived as the basis signal through the application of DWT on the EEG signal contaminated by artifacts. The signal is given to the ANC reference input. Since this EOG artifact is not regenerated well [22], the explicit diminution of this predicted signal from the EEG signal does not result in removal of all of the EOG elements from the corrupted EEG signal. To eliminate any remaining traces of EOG artifact, DWT is united with MEE. Finally, the MEE-based ANC accomplishes the removal of the EOG artifact through continuous adaptation of filter coefficients.

The structure of ANC, DWT, and the entropy-based error metric are elaborated upon in the second part of this study. Detailed description about the proposed method is provided in section 3. The analysis of simulations is provided in section 4. Finally, the conclusion is in section 5.

2. METHOD

In this section, the proposed method for EEG signal noise cancellation has been introduced. In this section, the structure of the adaptive noise cancellation is introduced and input-output signals are specified. Then, the weight updating algorithm for adaptive filter, based on the error entropy minimization is introduced that called MEE algorithm. Also, the mathematical equations of updating the weights are expressed. After that, the DWT transformation and its mathematical relationships are examined. Finally, the structure of the proposed method named DWT-ANC-MEE and how it works will be described.

2.1. Adaptive noise cancellation

The primary elements of ANC consist of blocks responsible for weight updates and filtering, as illustrated in Figure 1. Various algorithms, such as LMS, recursive least squares (RLS), or MEE, can be employed to update the weights. In our proposed approach, we opt for MEE owing to its exceptional capability to effectively track non-Gaussian and non-stationary noise, while also leveraging higher-degree statistical analysis. Using the presented method, the filter coefficients reach their optimum values with a reduced number of iterations in comparison to alternative techniques [3].

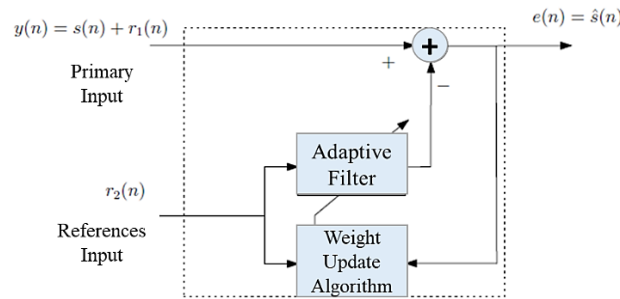


Figure 1. Overview of ANC configuration

2.2. Minimum error entropy method

The measure of average data content within a specific data arrangement is commonly referred to as the concept of entropy. Indeed, MSE represents a specific instance of entropy, as MSE exclusively deals with the second-order statistics of the error PDF, whereas entropy encompasses the entirety of the PDF of the error distribution. In fact, when entropy is minimized, all the moments of error distribution are minimized, not just the second moment. Therefore, the entropy criterion can be chosen as a better alternative to MSE. In this study, we employ the following extended definitions of entropy to offer versatility within a parametric set, with Shannon's concepts serving as the specific situation when the parameter 'a' equals 1. The Renyi entropy of 'e,' with order 'a,' is defined as (1) [18]:

$$H_{\alpha}(e) = \frac{1}{1-\alpha} \log \int f^{\alpha}(e) de \quad (1)$$

Here, $f(e)$ represents error random variable's PDF. In the present research, we have opted for Second-order Renyi's entropy denoted as $\alpha = 2$, which is expressed as (2):

$$H_2(e) = -\log \int f^2(e) de \quad (2)$$

As evident from (1) and (2), the computation of entropy necessitates knowledge of the PDF of a random variable. Consequently, in this study, the Parzen windowing method is employed for the estimation of this PDF. The Parzen windowing technique is represented by (3):

$$\hat{f}(e) = \frac{1}{N} \sum_{i=1}^N k_{\sigma}(e - e(i)) \quad (3)$$

Here, $k(e)$ represents the Kernel function, σ denotes the Kernel size, and $\{e(1), e(2), \dots, e(N)\}$ represents the error data points. While various kernel functions can be employed for the Parzen window, in this study, we utilize a multidimensional Gaussian distribution function with a radially symmetrical variance of σ^2 . Consequently, the estimation of Renyi's quadratic entropy for error samples is calculated as follows:

$$\begin{aligned}
\hat{H}_2(e) &= -\log \int_{-\infty}^{+\infty} \left(\frac{1}{N} \sum_{i=1}^N G_{\sigma}(e - e(i)) \right)^2 de \\
\hat{H}_2(e) &= -\log \frac{1}{N^2} \int_{-\infty}^{+\infty} \left(\sum_{i=1}^N \sum_{j=1}^N G_{\sigma}(e - e(j)) G_{\sigma}(e - e(i)) \right) de \\
\hat{H}_2(e) &= -\log \frac{1}{N^2} \left(\sum_{i=1}^N \sum_{j=1}^N \int_{-\infty}^{+\infty} G_{\sigma}(e - e(j)) G_{\sigma}(e - e(i)) de \right)
\end{aligned} \tag{4}$$

$$\hat{H}_2(e) = -\log \left(\frac{1}{N^2} \sum_{i=1}^N \sum_{j=1}^N G_{\sigma\sqrt{2}}(e(j) - e(i)) \right) \tag{5}$$

In (4) and (5), $G_{\sigma}(\cdot)$ represents the kernel function with a Gaussian core. The term enclosed within the logarithmic function, often referred to as information potential (IP), is presented as (6):

$$\hat{V}_2(e) = \frac{1}{N^2} \sum_{i=1}^N \sum_{j=1}^N G_{\sigma\sqrt{2}}(e(j) - e(i)) \tag{6}$$

Hence, the entropy equation for the error random variable can be expressed as (7):

$$\hat{H}_2(e) = -\log(\hat{V}_2(e)) \tag{7}$$

As the logarithm function is a monotonic transformation, it may be deduced that the lowest entropy corresponds to the highest IP. Then, the cost function $J(e)$ for the MEE criterion can be defined as (8):

$$J_{MEE}(e) = \max_w V(e) \tag{8}$$

In online training scenarios, the stochastic information gradient (SIG) can be employed to estimate the IP, as depicted in (9). As a common result, the stochastic gradient of information is derived, computed as the summation of L new samples at time n .

$$\hat{V}_2(e(n)) \approx \frac{1}{L} \sum_{i=n-L}^{n-1} G_{\sigma\sqrt{2}}(e(n) - e(i)) \tag{9}$$

By implementing the MEE-SIG method for coefficient updates, as described in [21], the aim is to reduce the signal $e(n)$ entropy within the adaptive filter illustrated in Figure 1.

$$W(n+1) = W(n) + \mu \cdot \nabla V(e(n)) \tag{10}$$

In this context, the gradient is calculated as (11):

$$\nabla V(e(n)) = \frac{1}{2\sigma^2 L} \sum_{i=n-L}^{n-1} G_{\sigma\sqrt{2}}(e(n) - e(i)) \{e(n) - e(i)\} \{X(n) - X(i)\} \tag{11}$$

2.3. Discrete wavelet transform

The wavelet analysis is among the most powerful tools for capturing both temporal and spectral information within a signal. It excels in providing enhanced temporal resolution for segments with higher frequencies and improved frequency resolution for components with lower frequencies. The signal, denoted as $y(t)$, could be expressed through a wavelet analysis as outlined in [23].

$$y(t) = \sum_m a_{Mm} \phi_{Mm} + \sum_{l=1}^M \sum_m d_{lm} \phi_{lm}(t) \tag{12}$$

Where a_{Mm} is the proximate and d_{lm} are the coefficients detail. To reconstruct the primary signal $y(t)$ at presented decomposition level (e.g., M), the process is as (13):

$$y(t) = A_M(t) + \sum_{l=1}^M D_l(t) \tag{13}$$

2.4. Proposed discrete wavelet transform-adaptive noise cancellation-minimum error entropy technique

Figure 2 depicts the process of EOG artifact cancellation using the DWT-MEE technique. The corrupted EEG signal $y(n)$, obtained as the sum of the EEG signal $s(n)$ and a constant ratio (p) of the EOG signal $r_1(n)$, is the input. To generate the reference signal required for the ANC, the DWT is employed on the signal vector $y = [y(1), y(2), \dots, y(N)]$, which is held in a buffer of size n . The subsequent subsections will detail the primary steps involved in creating the source signal for ANC.

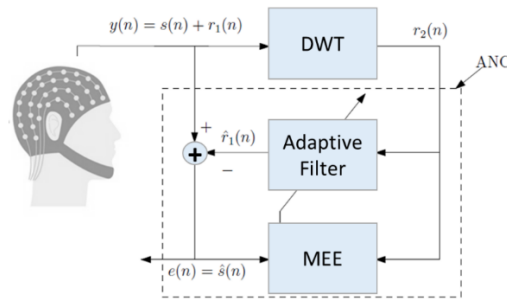


Figure 2. DWT-MEE method block diagram

2.4.1. Extraction the source signal for adaptive noise cancellation using discrete wavelet transform

In this study, we have conducted a multi-level wavelet decomposition using DWT up to level 8. This process enables the precise identification of wavelet coefficients associated with the EOG artifact, taking into consideration the effective factors such as eye movement (0-7 Hz) and blinking (8-13 Hz) (level 8: 0.25-0.5 Hz, level 7: 0.5-1 Hz, level 6: 1-2 Hz, level 5: 2-4 Hz, level 4: 4-8 Hz, level 3: 8-16 Hz, level 2: 16-32 Hz, and level 1: 32-64 Hz). Thresholding has been applied to the detail coefficients from level 8 down to level 3 for EOG denoising. Decomposing the EEG signal to level 3 provides the essential ocular-related wavelet coefficients necessary for noise reduction, as indicated in [24]. To obtain the reference signal, we apply the DWT to the noisy signal, resulting in the EOG signal vector, denoted as r_2 , which serves as the primary input for the ANC system.

2.4.2. Discrete wavelet transform-minimum error entropy

In the DWT-MEE method proposed, the ANC system takes as its initial and source inputs the contaminated EEG signal vector (y) and the elicited EOG signal vector (r_2), respectively. By renewing the coefficients of the filter using the MEE method, an estimate of the signal $\hat{r}_1(n)$ is obtained from the signal r_2 . To obtain a clean EEG signal, in each block of data, the estimated signal $\hat{r}_1(n)$ is deducted from the corrupted EEG signal $y(n)$. The time required to derive the corrected EEG signal for each block matches the combined computing durations of the serial-to-parallel converter, the DWT process, parallel-to-serial converter, and the ANC operation. This method is particularly advantageous as the computational time to obtain the accurate EEG signal is shorter than the sampling interval of the EEG signal.

3. RESULTS AND DISCUSSION

Deleting the EOG artifact from live EEG data allows researchers to test how well the proposed approach works. Even more so at frontal sites, the EEG signal might be contaminated by EOG artifact. Careful instructions can reduce the severity of the problem, but they rarely eliminate it entirely. Figure 3 shows a sample of experimental signals obtained from BCI competition dataset that used in the experiments. As can be seen the original EEG data shows in Figure 3(a). Also Figure 3(b) displays EOG artifact and Figure 3(c) represent signal contaminated with noise. A clean EEG signal, EOG artifact, and an EEG signal corrupted with EOG artifact can be seen in this figure. Also, in order to see the frequency spectrum of the clean signal, the EOG artifact and the corrupted EEG signal with the EOG artifact, their power spectral density (PSD) are shown in Figures 4(a) to 4(c) respectively. In this figure, the horizontal axis represents frequency and the vertical axis represents PSD.

Multiple EEG signal recordings covering a wide variety of wave shapes have been used to validate the proposed technique in the 2008 BCI competition dataset [25]. We have employed real-world EOG signal artifacts from a database utilized in the BCI competition in order to assess the enhancement performance within a dynamic environment. BCI datasets typically consist of three EOG channels and twenty-two EEG monopolar channels. All signals were bandpass filtered between 0.5 and 100 Hz and captured at 250 Hz. Additionally, a notch filter with a frequency of 50 Hz was used on this data set. Nine healthy volunteers were used to collect EEG data over the course of two sessions. Each session begins with three tasks: one with eyes closed, one with eyes open, and one including eye movements [25]. Compared to Croft's intended strategy [26], the electrode placement for the EOG signals in this data set is unique. All EEG signals were also filtered with a low-pass filter set at 45 Hz for this study. To avoid confounding the EEG readings, a low-pass filter set at 20 Hz is used to the EOG readings in this method [26]. Figure 3(b) depicts an EOG artifact, which we used as the model's reference signal $x(n)$. The input to an adaptive filter is an EEG signal that has been contaminated by EOG artifacts. In the

suggested technique, the PSD, coherence examination and signal-to-noise ratio (SNR) were used to assess the quality of noisy EEG signals. The equation for enhancing the quality of an EEG signal is as (14):

$$SNR = 10 \log_{10} \frac{\text{Var}(eeg_c(n))}{\text{Var}(eeg_c(n) - \widehat{eeg}_t(n))} \quad (14)$$

The variance operator is denoted by var, and the real $eeg_c(n)$ signal, and the true EEG signal $\widehat{eeg}_t(n)$ which is estimated using the adaptive filter, respectively.

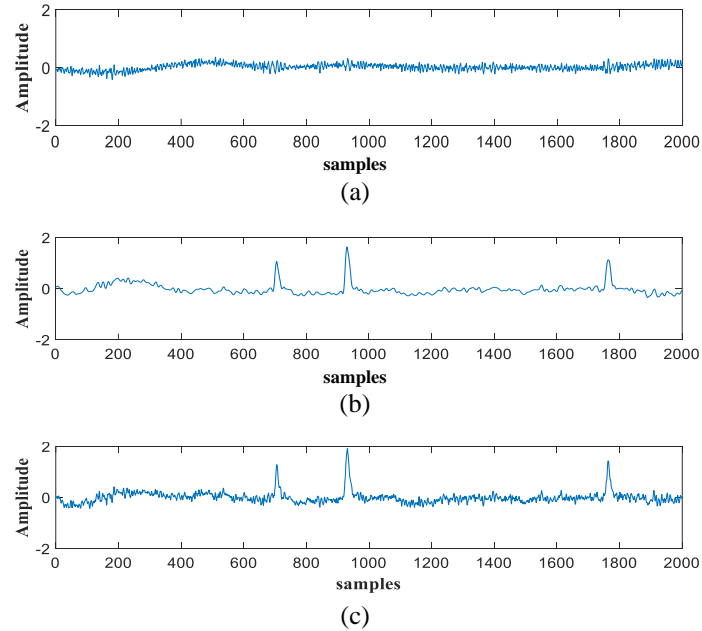


Figure 3. A sample of experimental signals from BCI competition dataset (a) EEG without noise, (b) EOG artifact, and (c) signal contaminated with noise

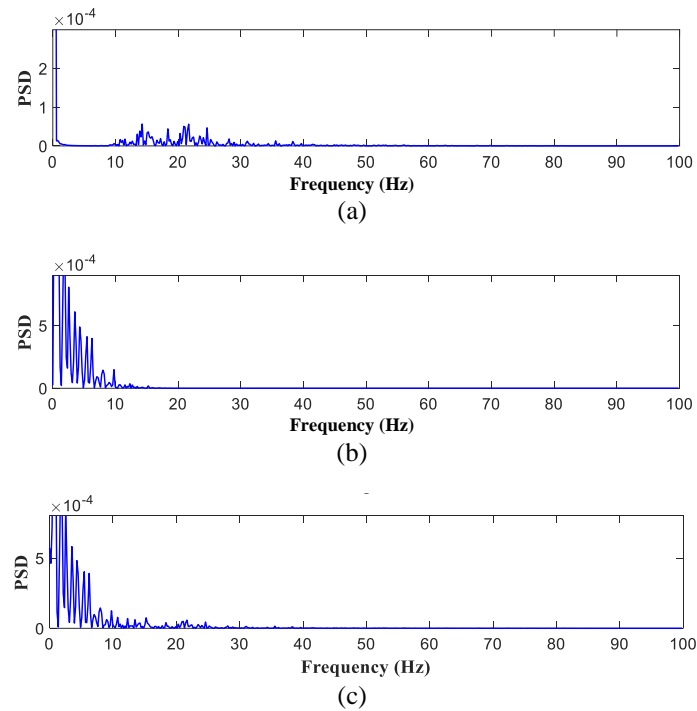


Figure 4. PSD of experimental signals (a) EEG signal, (b) EOG, and (c) EEG contaminated by EOG

Since the EEG signal is not constant, this article employs Welch's approach to estimate the power component using a Hamming-window of 1024 data points of 1 second duration with 50% overlap. We assessed spectral coherence between denoised and clean EEG signals as a numerical measurement for the proposed efficient denoising approach at the target frequency. The following is the consistency equation between the $\widehat{eeg}_t(f)$ signal and the $eeg_c(f)$ signal.

$$Coh(f) = \frac{|P_{eeg_c \widehat{eeg}_t}(f)|^2}{P_{eeg_c}(f) P_{\widehat{eeg}_t}(f)} \quad (15)$$

The cross-spectral density between signals $eeg_c(f)$ and $\widehat{eeg}_t(f)$ is represented by $P_{eeg_c \widehat{eeg}_t}(f)$, where $P_{eeg_c}(f)$ and $P_{\widehat{eeg}_t}(f)$ are the corresponding auto spectra.

Table 1 displays the results of a comparison between LMS-based and MEE-based algorithms applied to five separate recordings of electroencephalographic (EEG) activity. As can be seen in this table the SNR of the de-noised EEG signal averages at 3.32 dB when applying the LMS method and rises to 4.72 dB when utilizing mee method. These results show the significant superiority of the MEE algorithm over the LMS algorithm in terms of improving the SNR rate.

Table 1. Comparing the SNR between the LMS and the MEE methods

	SNR out (dB)		RMSE	
	DWT_LMS	DWT_MEE	DWT_LMS	DWT_MEE
Subject 1	0.42	1.69	0.10	0.09
Subject 2	2.60	2.98	0.15	0.14
Subject 3	5.87	6.52	0.11	0.10
Subject 4	2.27	5.25	0.30	0.21
Subject 5	5.44	7.16	0.15	0.12
Average	3.32	4.72	0.16	0.13

The findings illustrate that the MEE approach surpasses the LMS algorithm in effectively removing the EOG artifact. Our calculations in this paper are based on a dataset of 2000 EEG samples, employing a step size coefficient (μ) of 0.01 in LMS and a value of 1 for MEE. Additionally shown are the outcomes of a simulated EEG with a signal-to-noise ratio of -2 dB due to contamination. Figure 5 displays the effectiveness of the MEE and LMS algorithms in removing noise. Figure 5(a) shows denoised signal using DWT-LMS algorithm and Figure 5(b) shows denoised signal using DWT-MEE method. In addition, Figure 6 showcases the PSD both prior to and following filtration using the LMS and MEE algorithms. Figure 6(a) shows PSD of contaminated EEG. Also Figure 6(b) represent filtered PSD with LMS, and Figure 6(c) display filtered PSD using MEE method.

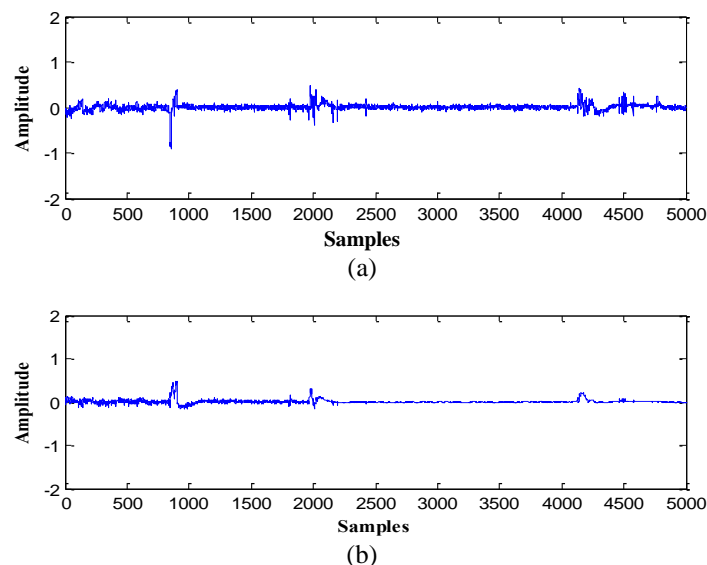


Figure 5. Denoising results: (a) denoised using DWT-LMS algorithm, and (b) denoised using DWT-MEE method

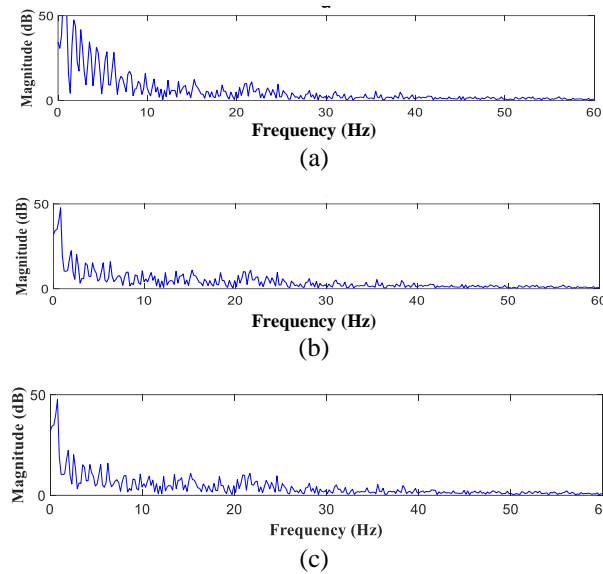


Figure 6. PSD before and after filtration (a) PSD of contaminated EEG, (b) filtered PSD with LMS, and (c) filtered PSD using MEE method

Figure 7 represents the progression of MEE and LMS techniques as well as the disparities in the reconstructed and clean signal. Figure 7(a) displays the outcomes of EOG removal with the LMS algorithm, and Figure 7(b) shows the outcomes of EOG removal with the MEE method. The results show that the MEE algorithm outperforms the LMS algorithm at reducing steady-state error. Also coherence of the original and reconstructed signals employing ANC filter with LMS, and MEE algorithm are displayed in Figures 8(a) and 8(b), respectively. Substituting the error entropy criterion for the MSE criterion demonstrates a general improvement in coherence values, particularly in the lower frequency range.

In conclusion, we utilize the relative root mean square error (RRMSE) criterion to assess and compare the effectiveness of this approach against other recently introduced methods. RRMSE is calculated as (16):

$$RRMSE = \frac{RMS(S-\hat{S})}{RMS(S)} \quad (16)$$

In the (16), the root mean square of the original signal denoted as $RMS(S)$, while $RMS(\hat{S})$ denotes the root mean square of cleaned EEG signals.

Figure 9 illustrates an effectiveness comparison of proposed approach using SSA-ANC and the method from [27], DWT-ANC, with regard to the RRMSE metric. In this figure, the horizontal axis shows the SNR and the vertical axis shows the RRMSE in percent. As can be seen in the figure, the method presented in this work in all SNRs has a lower RRMSE than other methods, which indicates the better performance of the method presented in all SNRs. For example, in SNR equal to 2, the RRMSE criterion for the proposed DWT-ANS-CMEE method is equal to 46, which is 41% superior to the SSA-ANC-RLS algorithm. This shows the effectiveness of the proposed method in conditions with high noise power (low SNRs).

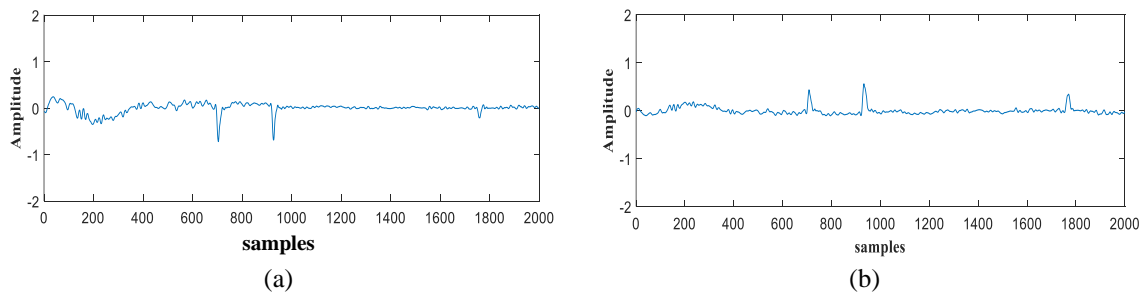


Figure 7. The error signals after denoising: (a) the outcomes of EOG removal with the LMS algorithm, and (b) the outcomes of EOG removal with the MEE method

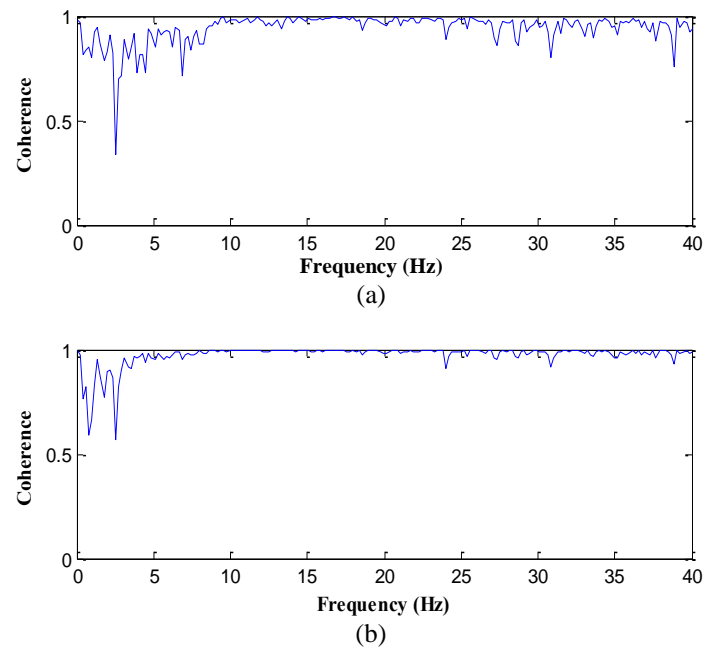


Figure 8. The consistency between the primary and recreated signals: (a) outcomes of EOG removal using the LMS method and (b) outcomes of EOG removal using the MEE method

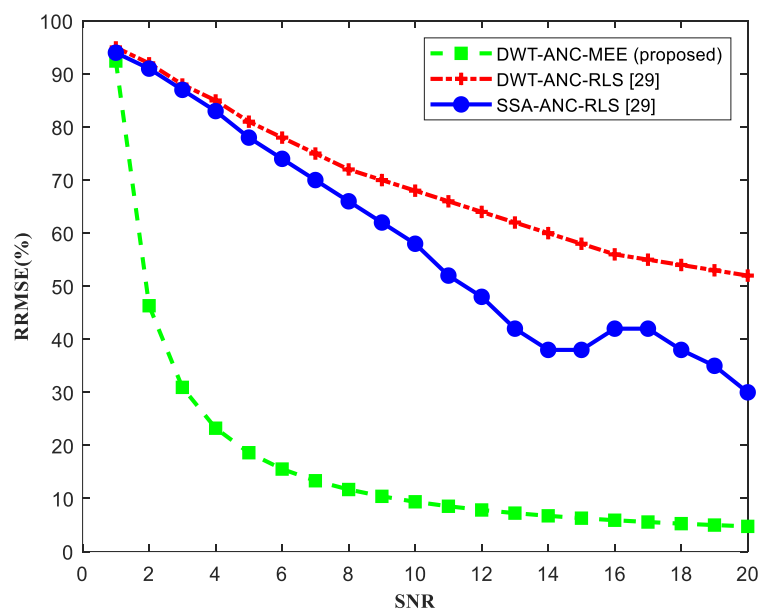


Figure 9. Evaluation of the SSA-ANC and DWT-ANC methods in relation to RRMSE

It is worth mentioning that this research has investigated simultaneously all the criteria of RRMSE criteria, output SNR after filtering, error amplitude curve after denoising operation, PSD and coherence analyses. While previous studies have not investigated the simultaneous effect of all these criteria, and previous studies have investigated some of these criteria. we found that the output SNR measure were correlated with the RMSE measure. The proposed method in this study tends to have an extremely low ratio of RMSE compared to other previous studies which confirms the reduction of filtration error in the proposed method. Our study suggests that lower RMSE is not associated with poor performance in output SNR. The proposed method may benefit from RMSE without adversely on output SNR of denoised signal. in this paper a comprehensive study in EEG signal noise removal with DWT-ANC-MEE algorithm explored. However, further and in-depth studies may be needed to confirm its effectiveness on more samples of EEG signals. In

this study, it was shown that denoising algorithms based on error entropy are more efficient than traditional methods for denoising the EEG signal. Future studies may investigate more up-to-date adaptive algorithms for denoising the EEG signal. Recent observations in EEG signal denoising studies show that adaptive filtering methods can provide appropriate performance in EEG signal denoising with low error rates. Our findings provide conclusive evidence that proper updating of the adaptive filter coefficients using the MEE algorithm can lead to better performance of the ANC system. The results obtained in this work confirm this issue.

4. CONCLUSION

This paper introduces a hybrid approach employing both DWT and ANC for the extraction of EOG artifacts from EEG signals. The methodology leverages DWT to derive an approximation of the EOG signal, which serves as the basis input for the adaptive filter. Furthermore, use of the MEE algorithm is advocated for noise reduction within the adaptive system, particularly for non-Gaussian signals, where it demonstrates superior suitability compared to MSE-based algorithms. A performance evaluation of the proposed system against MSE-based algorithms reveals its superior performance in metrics such as RRMSE, SNR of output, and coherence analyses.




REFERENCES

- [1] D. Gorjan, K. Gramann, K. D. Pauw, and U. Marusic, "Removal of movement-induced EEG artifacts: Current state of the art and guidelines," *Journal of Neural Engineering*, vol. 19, no. 1, 2022, doi: 10.1088/1741-2552/ac542c.
- [2] J. Yin, A. Liu, C. Li, R. Qian, and X. Chen, "Frequency information enhanced deep EEG denoising network for ocular artifact removal," *IEEE Sensors Journal*, vol. 22, no. 22, pp. 21855–21865, 2022, doi: 10.1109/JSEN.2022.3209805.
- [3] A. Darroudi, J. Parchami, K. Razavi, and G. Sarbisheie, "EEG adaptive noise cancellation using information theoretic approach," *Bio-Medical Materials and Engineering*, vol. 28, no. 4, pp. 325–338, 2017, doi: 10.3233/BME-171680.
- [4] V. Srivastava, "An optimization for adaptive multi-filter estimation in medical images and EEG based signal denoising," *Biomedical Signal Processing and Control*, vol. 82, 2023, doi: 10.1016/j.bspc.2022.104513.
- [5] V. Dalal and S. Bhairannawar, "Efficient de-noising technique for electroencephalogram signal processing," *IAES International Journal of Artificial Intelligence*, vol. 11, no. 2, pp. 603–612, 2022, doi: 10.11591/ijai.v11.i2.pp603-612.
- [6] A. Darroudi, J. Parchami, G. Sarbisheie, and S. Rajan, "Removing ECG noise from surface EMG based on information theory," in *Electrical Engineering (ICEE), Iranian Conference on*, 2018, pp. 1403–1408, doi: 10.1109/ICEE.2018.8472613.
- [7] C. S. L. Prasanna and M. Z. U. Rahman, "A reference free non-negative adaptive learning system for health care monitoring and adaptive physiological artifact elimination in brain waves," *Healthcare Analytics*, vol. 4, p. 100225, 2023, doi: 10.1016/j.health.2023.100225.
- [8] N. Ansari, Y. U. Khan, A. T. Khan, and O. Farooq, "Automatic removal of ocular and cardiac artifacts and retention of embedded EEG information via adaptive noise cancellation," in *2023 International Conference on Recent Advances in Electrical, Electronics & Digital Healthcare Technologies (REEDCON)*, 2023, pp. 133–138, doi: 10.1109/REEDCON57544.2023.10151101.
- [9] S. Sharma and U. Satija, "Automated ocular artifacts removal framework based on adaptive chirp mode decomposition," *IEEE Sensors Journal*, vol. 22, no. 6, pp. 5806–5814, 2022, doi: 10.1109/JSEN.2022.3147010.
- [10] J. Yedukondalu and L. D. Sharma, "Circulant singular spectrum analysis and discrete wavelet transform for automated removal of EOG artifacts from EEG signals," *Sensors*, vol. 23, no. 3, 2023, doi: 10.3390/s23031235.
- [11] A. Bhattacharyya, A. Verma, R. Ranta, and R. B. Pachori, "Ocular artifacts elimination from multivariate EEG signal using frequency-spatial filtering," *IEEE Transactions on Cognitive and Developmental Systems*, vol. 15, no. 3, pp. 1547–1559, 2023, doi: 10.1109/TCDS.2022.3226775.
- [12] A. K. Maddirala and K. C. Veluvolu, "SSA with CWT and k-means for eye-blink artifact removal from single-channel EEG signals," *Sensors*, vol. 22, no. 3, 2022, doi: 10.3390/s22030931.
- [13] H. Hu, Z. Pu, and P. Wang, "A flexible and accurate method for electroencephalography rhythms extraction based on circulant singular spectrum analysis," *PeerJ*, vol. 10, 2022, doi: 10.7717/peerj.13096.
- [14] C. M. Bishop, *Neural networks for pattern recognition*. Oxford, United Kingdom: Clarendon Press, 1995.
- [15] M. T. Akhtar, W. Mitsuhashi, and C. J. James, "Employing spatially constrained ICA and wavelet denoising, for automatic removal of artifacts from multichannel EEG data," *Signal Processing*, vol. 92, no. 2, pp. 401–416, 2012, doi: 10.1016/j.sigpro.2011.08.005.
- [16] S. Sanei, T. K. M. Lee, and V. Abolghasemi, "A new adaptive line enhancer based on singular spectrum analysis," *IEEE Transactions on Biomedical Engineering*, vol. 59, no. 2, pp. 428–434, 2012, doi: 10.1109/TBME.2011.2173936.
- [17] H. Abdollahniya, A. A. Khazaei, and M. Azarnoosh, "A DWT-ANC error entropy criterion based single-channel EEG signal EOG noise reduction," *International Journal of Nonlinear Analysis and Applications*, vol. 14, pp. 667–677, 2023, doi: 10.22075/ijnaa.2022.26474.3326.
- [18] D. Erdogmus and J. C. Principe, "An error-entropy minimization algorithm for supervised training of nonlinear adaptive systems," *IEEE Transactions on Signal Processing*, vol. 50, no. 7, pp. 1780–1786, 2002, doi: 10.1109/TSP.2002.1011217.
- [19] M. Li, Z. Jing, and H. Leung, "Robust minimum error entropy based cubature information filter with non-gaussian measurement noise," *IEEE Signal Processing Letters*, vol. 28, pp. 349–353, 2021, doi: 10.1109/LSP.2021.3055748.
- [20] S. Han, S. Rao, D. Erdogmus, and J. Principe, "An improved minimum error entropy criterion with self adjusting step-size," in *2005 IEEE Workshop on Machine Learning for Signal Processing*, 2005, pp. 317–322, doi: 10.1109/MLSP.2005.1532921.
- [21] C. Safarian and T. Ogunfunmi, "Quaternion kernel normalized minimum error entropy adaptive algorithms," in *2018 Asia-Pacific Signal and Information Processing Association Annual Summit and Conference (APSIPA ASC)*, 2018, pp. 572–578, doi: 10.23919/APSIPA.2018.8659787.
- [22] M. K. Yadavalli and V. K. Pamula, "An efficient framework to automatic extract EOG artifacts from single channel EEG recordings," in *2022 IEEE International Conference on Signal Processing and Communications (SPCOM)*, 2022, pp. 1–5, doi: 10.1109/SPCOM55316.2022.9840849.
- [23] B. Azzerboni, M. Carpentieri, F. L. Foresta, and F. C. Morabito, "Neural-ICA and wavelet transform for artifacts removal in surface




- EMG,” *IEEE International Conference on Neural Networks - Conference Proceedings*, vol. 4, pp. 3223–3228, 2004, doi: 10.1109/ijcnn.2004.1381194.
- [24] S. Khatun, R. Mahajan, and B. I. Morshed, “Comparative study of wavelet-based unsupervised ocular artifact removal techniques for single-channel EEG data,” *IEEE Journal of Translational Engineering in Health and Medicine*, vol. 4, pp. 1–8, 2016, doi: 10.1109/JTEHM.2016.2544298.
- [25] C. Brunner, R. Leeb, and G. Müller-Putz, “BCI Competition 2008 – Graz dataset IIA,” *IEEE Dataport*, pp. 1–6, 2008, doi: 10.21227/katb-zv89.
- [26] R. J. Croft and R. J. Barry, “Removal of ocular artifact from the EEG: A review,” *Neurophysiologie Clinique*, vol. 30, no. 1, pp. 5–19, 2000, doi: 10.1016/S0987-7053(00)00055-1.
- [27] A. Maddirala and R. A. Shaik, “Removal of EOG artifacts from single channel EEG signals using combined singular spectrum analysis and adaptive noise canceler,” *IEEE Sensors Journal*, vol. 16, no. 23, 2016, doi: 10.1109/JSEN.2016.2560219.

BIOGRAPHIES OF AUTHORS






Hashem Abdolahniya    is a lecturer in the Department of Electrical Engineering at Azad University of Mashhad. He is currently a Ph.D. student at Mashhad Azad University in Mashhad. His research interests include signal processing, medical image processing, noise removal, adaptive filters, and image compression. He can be contacted at email: hashem.abdolahniya@yahoo.com.






Dr. Ali Akbar Khazaei    was born in Mashhad, Iran on May 09, 1969. He received his B.S. degree in electronics engineering from Ferdowsi University of Mashhad in 1992, his M.Sc. in communication engineering from Tarbiat Modares University, Tehran, Iran, in 1996 and his Ph.D. in communication engineering from Islamic Azad University, Science and Research Branch, Tehran, Iran, in 2012 respectively. From 2008 to 2012 he was with the Satellite Communication Group, Iran Telecommunication Research Center (ITRC), Tehran, Iran. He has been with the Department of Electrical Engineering of Islamic Azad University, Mashhad, Iran, as an Assistant Professor from 2012 to now. He can be contacted at email: khazaei@mshdiau.ac.ir.



Dr. Mahdi Azarnoosh    is an Assistant Professor of medical engineering at Islamic Azad University, Mashhad Branch. He received his doctorate in the field of medical/bioelectrical engineering at Tehran Islamic Azad University of Science and Research. His research interests include: acquisition, processing, and analysis of vital signals. He can be contacted at email: m_azarnoosh@mshdiau.ac.ir.



Dr. Seyed Ehsan Razavi    received his B.Sc. in electrical engineering (2006), M.Sc. in control engineering (2008), and Ph.D. in control engineering (2014). Currently, he is an Associate Professor at the Department of Electrical Engineering, Islamic Azad University of Mashhad. His current research interests are control theory, biomedical engineering, nanoparticles, image processing and hyperthermia. He has authored several book chapters and published more than 30 papers in journals and conferences. He can be contacted at email: ehsanrazavi@mshdiau.ac.ir.